

## **Phenol Removal From Wastewater By Oxidation Method Using Zeolite Prepared Locally**

<p><i>Lec.</i>  <b>Mohammed Nsaif Abbas</b>  <i>Al-Mustansiriya University</i>  <i>College of Engineering</i>  <i>Environmental Eng. Dep.</i>  <a href="mailto:mohammed.nsaif@yahoo.com">mohammed.nsaif@yahoo.com</a>  <u>om</u></p>	<p><i>Assist. Lec</i>  <b>Hala Husham Nussrat</b>  <i>Al-Mustansiriya University</i>  <i>College of Engineering</i>  <i>Environmental Eng. Dep.</i>  <a href="mailto:hala_husham@yahoo.com">hala_husham@yahoo.com</a></p>	<p><i>Assist. Lec</i>  <b>Safaa Nemat Hussein</b>  <i>Al-Mustansiriya University</i>  <i>College of Engineering</i>  <i>Environmental Eng. Dep.</i>  <a href="mailto:safaadeeb@yahoo.com">safaadeeb@yahoo.com</a></p>
--	---	---

### **ABSTRACT :**

*A customary method to oxidize phenol, present in wastewater, was developed by using oxidation method in the presence of local faujasite type Y – zeolite catalyst prepared from Iraqi rice husk as a silica source and studying the behavior of this catalyst in a continuous bed reactor to remove phenol from hospital wastewater experimentally and theoretically by oxidation method. Experimental part of this investigation involved oxidize reaction of phenol, which was carried out using the above prepared catalyst at different variables which were the reaction temperature, weight hourly space velocity (WHSV), oxygen partial pressure, pH of feed solution, phenol initial concentration, catalyst bed height and gas flow rate were varied from (100–200°C), (1–5 h<sup>-1</sup>), (5–15 bar), (3–11), (2–10 mg/l), (40–80) cm and (20–100%) stoichiometric excess respectively. The analysis of phenol remaining in samples produced from oxidation reaction was achieved using spectrophotometer equipment. In the theoretical part, Equilibrium and Rate Based or Nonequilibrium mathematical models were developed using MATLAB and FORTRAN simultaneously to solve MESH equations, M: Material Balance, E: Equilibrium Relations, S: Summation Equations, H: Heat Balance and R: Reaction Equations. Rate Based model was developed dependence on Equilibrium model results and taking into account the effect of mass and heat transfer on material and energy balances. The general behavior of oxidation process indicates that phenol conversion increased with increasing temperature of reaction, oxygen partial pressure, gas flow rate, pH of feed solution, and height of catalyst bed while decreased with increasing pH, Weight Hourly Space Velocity (WHSV) and initial concentration of phenol. The conversion of phenol during oxidation process was 98.79 % using faujasite type Y– zeolite catalyst. The Kinetic results exhibit that the reaction is first and half orders with respect to phenol and oxygen respectively while the activation energy observed was 79.91 kJ/mol. The results of experimental work compared with the results obtained from the developed program of Rate Based or Nonequilibrium model and the deviation shows distinct approximation in results with negligible error. Statistical model was also implemented to find a general expression relates all parameters used in this investigation in one equation. By this way we can remove the toxic phenol from hospital waste-water which was one of the materials that contaminated the water using a catalyst prepared from cheap material (IRH) and discarding it in a cost and eco-friendly method.*

*Key words: Phenol Removal, Wastewater, Oxidation and Type Y– Zeolite Catalyst*

## إزالة الفينول من مياه المخلفات بطريقة الأكسدة باستخدام الزيولايت المحضر محلياً

صفاء نعمت حسين

هالة هشام نصرت

محمد نصيف عباس

## الخلاصة :

تعتبر طريقة الأكسدة من الطرق الشائعة والمألوفة للتخلص من الفينول الموجود في مياه المخلفات ، تم في هذا البحث تطوير هذه الطريقة للتخلص من الفينول الموجود في المياه المتخلفة من المستشفيات باستخدام العامل المساعد الفوجاسايت زيولايت نوع - Y المحضر محلياً من قشور الرز العراقي كمصدر للسليكا ودراسة سلوك هذا العامل المساعد في منظومة العمود المستمر لإزالة الفينول من مخلفات مياه المستشفيات عملياً ونظرياً بطريقة الأكسدة . تناول الجزء العملي من هذا البحث دراسة تفاعل أكسدة الفينول والذي تم باستخدام العامل المساعد المحضر أعلاه وبتأثير عوامل مختلفة هي درجة حرارة التفاعل ، والسرعة الفراغية الوزنية ، والضغط الجزئي للأوكسجين ، وقيمة الدالة الحامضية للقيم الداخل إلى المنظومة ، وتركيز الفينول الابتدائي ، وإرتفاع طبقة العامل المساعد داخل مفاعل المنظومة ، ومعدل جريان الغاز وهذه العوامل كانت قد تغيرت من (100-200م)، (1-5 سا<sup>-1</sup>) ، (5-15 بار) ، (3-11) ، (2-10 مغم/لتر) ، (40-80) سم ، (20-100 % نسبة الزيادة المتناسبة) على التوالي . تم تحليل النماذج الناتجة من عملية الأكسدة لمعرفة تركيز الفينول المتبقي باستخدام الطريقة اللونية . في الجانب النظري تم تطوير موديل رياضي عند حالة التوازن و آخر عند حالة عدم التوازن باستخدام برنامج MATLAB ولغة FORTRAN سوية لحل معادلات توازن المادة والطاقة ولمحاكاة منظومة عملية الأكسدة أثناء حصول التفاعل . أظهرت النتائج العملية أن نسبة إزالة الفينول تزداد بزيادة درجة حرارة التفاعل ، والضغط الجزئي للأوكسجين ، وإرتفاع طبقة العامل المساعد ، ومعدل جريان الغاز وتقل نسبة الإزالة بزيادة السرعة الفراغية ، وتركيز الفينول الابتدائي ، والدالة الحامضية للقيم الداخل إلى المنظومة . وكانت أعلى نسبة تحول للفينول باستخدام هذا العامل المساعد هي 98.79 % . أظهرت دراسة حركية التفاعل ان التفاعل من المرتبة الأولى وأن طاقة تنشيطه باستخدام هذا عامل مساعد المحضر محلياً هي 79.91 كيلو جول/مول . وقد أظهرت النتائج المستحصلة من الموديل الرياضي نتائج متقاربة إلى حد كبير مع النتائج العملية وبنسبة خطأ قليلة جداً . تم في هذا البحث أيضاً إيجاد موديل إحصائي من خلال إيجاد معادلة عامة تربط جميع المتغيرات المستخدمة في البحث مع نسبة إزالة الفينول من المحاليل المائية . وبهذه الطريقة تم التخلص من أحد أخطر المواد السامة الموجودة في المياه المتخلفة من المستشفيات وباستخدام مادة رخيصة وليست ذات قيمة (وهي قشور الرز العراقي) وبطريقة إقتصادية وصديقة للبيئة .

## NOTATIONS

Symbol	Description	Unit
$a$	Interfacial Surface Area	$m^2/m^3$
$a, b, c, d$	Constants of Heat Capacity of Liquid Phase	-
$B^o, B'$	Varial Equation Constants	-
$C$	Concentration	$mol/m^3$
$C_a$	Capillary Number	-
$C_p$	Specific Heat	J/mol.K
$d$	diameter of the bed	m
$D$	Maxwell-Stefan diffusivity	$m^2/s$
$D^V$	Diffusivity of Vapour Mixture	$m^2/s$
$D^L$	Diffusivity of Liquid Mixture	$m^2/s$
$D^o_{ij,k}$	Diffusivity of Dilute Liquid Mixture	$m^2/s$
$D_e$	Effective Diffusivity	$m^2/s$

$d_p$	Particle diameter	m
$d_{pore}$	Pore diameter	nm
$e$	<b>Rate of Heat Transfer</b>	<b>J/s</b>
$E$	<b>Energy</b>	<b>J</b>
$E_a$	<b>Activation energy</b>	<b>kJ/mol</b>
$F$	Feed flow rate	mol/s
$f_o$	<b>Correction Factor</b>	–
$f$	Fugacity of Pure Component	kPa
$H^V$	Vapor mixture enthalpy	J/mol
$H^L$	Liquid mixture enthalpy	J/mol
$H_{mix}$	<b>Heat of Mixture</b>	<b>J/mol</b>
$\Delta H$	<b>Activation enthalpy</b>	<b>kJ/mol</b>
$H_r$	<b>Heat of Reaction</b>	<b>J/mol</b>
$\Delta H_b^V$	<b>Heat of Vaporization at Normal Boiling Point</b>	<b>kJ/mol</b>
$h^V$	Heat Transfer Coefficient in Vapour Phase	W/K
$h^L$	Heat Transfer Coefficient in Liquid Phase	W/K
$J$	<b>Diffusion Flux</b>	<b>mol/ m<sup>2</sup>.s</b>
$h$	<b>Plank's constant</b>	<b>6.63 × 10<sup>-24</sup> J/s</b>
$K$	Overall mass transfer coefficient	mol/(m <sup>2</sup> .mol.s)
$k$	First Order Reaction Rate Constant	s <sup>-1</sup>
$K_B$	<b>Boltzman constant</b>	<b>1.381 × 10<sup>-23</sup> J/K</b>
$L$	Liquid flow rate	mol/s
$M$	Molar holdup	mol
$N$	<b>Mass Transfer Rate</b>	<b>mol/s</b>
$N_{Le}$	Lewis Number	–
$N_{Pr}$	Prandtl Number	–
$P$	Pressure	kPa
$Q$	Heat load	J/hr
$E_R$	External reflux ratio	–
$r$	Reaction rate	mol/s
$R$	<b>Universal gas constant</b>	<b>8.314 J/mol.K</b>
$R_e$	<b>Reynolds Number</b>	–
$S$	Side stream flow rate	mol/s
$Sc$	<b>Schmidt Number</b>	–
$T$	Temperature	K
$t$	Time	s
$V$	Vapor flow rate	mole/s
$x$	Mole fraction in liquid phase	–
$y$	Mole fraction in vapor phase	–
$z$	<b>Mole Fraction in Feed Flow Rate</b>	–
$g$	Activity coefficient	–
$\varepsilon$	Packed bed voidage	–
$\eta$	Effectiveness Factor	–
$\eta$	Distance along diffusion path	<b>m</b>
$\mu$	Viscosity	<b>kg/m.s</b>
$\nu$	Stoichiometric Coefficient	–
$\rho$	Density	<b>g/cm<sup>3</sup></b>
$\tau$	Tortuosity	–
$\phi$	Fugacity Coefficient	–
$\varepsilon$	Reaction Volume	–
$\sigma$	Surface Tension	N/m

$\sigma_c$  Critical Surface Tension N/m

Superscript	Description
V	Vapor
L	Liquid
<sup>o</sup>	Reference
sat	saturation

## 1. INTRODUCTION :

There is growing concern about wide spread contamination of surface and ground water by various organic compounds due to the rapid development of chemical and petrochemical industries over the past several decades. These industries such as petrochemical, petroleum refining, chemical and pharmaceutical produce wastewater containing organic materials such as phenols, which are highly hazardous to aquatic life. The increasing release of concentrated toxic organic pollutions contained in many industrial end stream effluents has been the driving force for developing alternative effluent treatments prior to their discharge to conventional bio-filters or sewage plants. Therefore, many industrial wastes contain organics, which are difficult, or impossible to remove by conventional classical treatment processes <sup>[1,2]</sup>. The production of phenol has continuously grown for the last decades until reaching 1900 millions of kilograms in 1995 for the USA alone because it's used in the production of a wide range of consumer goods and materials such as; plasticizers, herbicides, insecticides, dyes, rubber chemicals, insulating foams, binders, adhesives and detergents <sup>[3]</sup>. Phenol as a class of organics is similar in structure the more common herbicides and insecticides in that they are resistant to biodegradation. Phenol is very soluble in water. The odor threshold for phenol is 0.04 ppm according to US Environmental Protection Agency (U.S.EPA). Their presence in water supplies are noticed as had taste and odor <sup>[4]</sup>. Phenols are considered as priority pollutants since they are harmful to organisms at low concentrations and many of them have been classified as hazardous pollutants because of their potential harm to human health. (U.S.EPA) Stringent (U.S.EPA) regulation call for lowering phenol content in the wastewater less than 1mg/L <sup>[5]</sup>. Thus, phenol and its derivatives, which are present in many wastewater streams, must be specifically treated before discarding the effluent for subsequent treatment in conventional sewage plants because of their extreme toxicity for aquatic life <sup>[6,7]</sup>. The application of a chemical oxidation method depends on, among other, the nature of the pollutant, the concentration of the pollutant, the desired removal efficiency, effectiveness, ability to form secondary toxic product and coast. Wet oxidation of organic compound to CO<sub>2</sub> and water represents a feasible approach to wastewater treatment. However, wet oxidation of wastewater without the aid of catalyst, is usually conducted to very high temperature and pressure (200-320°C and 70-200 bar) and operation costs <sup>[8]</sup>. In the last decades, catalytic oxidation using air or pure oxygen has received great attention because it is a suitable solution to the destruction of rather organic pollutants which provides milder operating conditions and more attractive process economics than wet air oxidation. Thus,

catalytic oxidation appears as an economically and ecologically promising technique to convert refractory organic compounds, such as phenol into carbon dioxide or harmless intermediates at mild pressure and temperature conditions<sup>[9]</sup>. The aim of this investigation were prepare zeolite types Y from IRH as a silica resource and tested the effect of changing operating conditions such as reaction temperature, weight hourly space velocity (WHSV), oxygen partial pressure, pH of feed solution, phenol initial concentration, height of catalyst bed and gas flow rate were stoichiometric excess on the of the phenol removal by oxidation in experimental unit to reach the best conditions for phenol removing from wastewater, and developed a simulation rate based or equilibrium model described the oxidation process and compare the results of experimental work with the theoretical results of simulation in rate based or non-equilibrium model.

## 2. EXPERIMENTAL WORK :

### 2.1 Catalyst Preparation :

#### 2.1.1 Iraqi rice husk (IRH) :

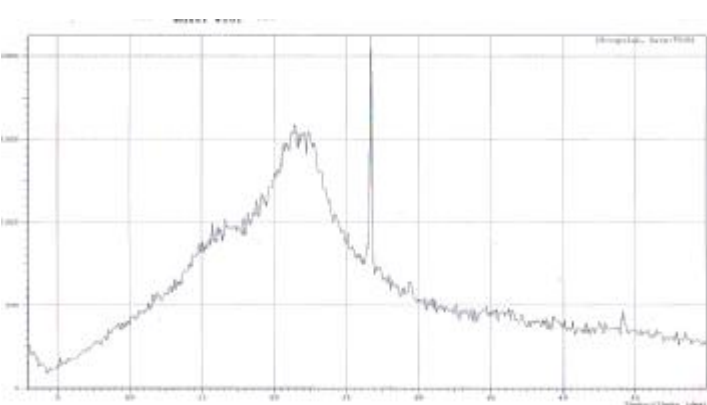
Iraqi rice husk was collected from Al-Shanafia fields for rice in the Southern of Iraq. The IRH was washed three times with doubled distilled water. Excess distilled water was used to remove the soluble materials present in the IRH bringing from the field, boiled to remove color and other fine impurities may be found in the IRH, and then dried at 105°C for 24 hours. The surface area of IRH was measured by BET nitrogen adsorption technique. When the IRH was heated at 105°C for 12 hours, most of the water had been removed from it while the second major mass loss of about 45-65% was attributed to the breakdown of cellulose constituent char. The IRH was treated with 10% sulfuric acid (H<sub>2</sub>SO<sub>4</sub>) for 24 hours for preliminary removing all impurities. Dry IRH were sieved to eliminate residual and clay particles. They were well washed with double distilled water, filtered, and calcined at 750°C for 6 hours. Twelve g of calcined IRH above were then subjected for dissolution in sodium hydroxide NaOH (4 M) followed by refluxing at 90°C for 12 hours. Concentrated (HCl (37%)) was then added to the aforementioned base dissolved IRH for complete precipitation. IRH were filtered, washed with excess distilled water to be freeing from chloride ions and finally dried in an oven at 105°C for 6 hours. The chemical composition and XRD of IRH is showed in **Table 1** all values in wt% basis<sup>[10,11]</sup>.

### 2.1.2 Preparation of Faujasite Type Y–Zeolite Catalyst from Iraqi Rice Husk :

Faujasite type Y– zeolite could be synthesized<sup>[10]</sup> using IRH as a silica source. Teflon beaker of 500 ml containing a magnetic stirrer was washed with deionized water. Sodium hydroxide of 1.6616 g was added slowly to deionized water and stir until clear and homogenous solution appeared for about 5 minutes. The aqueous solution of sodium hydroxide was ready for the preparation of seed gel. The gel was prepared according to the following molar chemical composition: **10.67 Na<sub>2</sub>O: 1 Al<sub>2</sub>O<sub>3</sub>: 10 SiO<sub>2</sub>: 180 H<sub>2</sub>O**.

Two milliliter aqueous solution of sodium hydroxide was added to 0.7515g sodium aluminate oxide until a homogenous mixture was formed; 1.5361 g IRH was added separately to 5.5 ml sodium hydroxide aqueous until homogeneously mixed. Both of the preparations were heated under vigorous stirring to obtain a homogenous mixture. The sample was aged for 24 hours at room temperature in the Teflon bottle. The aluminate and silicate solutions were mixed together in the polypropylene beaker, subsequently stirred for 2 hours with the purpose of making it completely homogenized. This combined solution was used as the feed stock gel. The flow chart of the process is shown in **Figure 1**.

**Table1: Iraqi Rice Husk Characterization**

Chemical Composition		XRD of Iraqi Rice Husk
Compound	Composition wt %	
SiO <sub>2</sub>	90.70	
Al <sub>2</sub> O <sub>3</sub>	0.13	
Fe <sub>2</sub> O <sub>3</sub>	0.06	
TiO <sub>2</sub>	0.015	
CaO	0.61	
MgO	0.25	
Na <sub>2</sub> O	0.09	
K <sub>2</sub> O	2.64	
P <sub>2</sub> O <sub>5</sub>	0.73	
LOI	4.71	
S.A (m <sup>2</sup> /g)	17.5	

### 2.1.3 Preparation of HY-Zeolite Catalyst :

The hydrogen zeolite form was prepared by exchanging Na<sup>+</sup> ions in the sodium form NaY-zeolite with ammonium chloride solution NH<sub>4</sub>Cl. In order to obtain ideal degree of ion exchange the technique of multi-steps (three times repeating) was used. Thus, the first step, 2 N of ammonium chloride solution (26.75 g of NH<sub>4</sub>Cl in 250 ml of distilled water) contacted with 90 g of faujasite type Y– zeolite (prepared above) with stirring for 2 hours. In the second step, the procedure in the first step was repeated under the same conditions but for 60 g of faujasite type Y-zeolite, which was taken from the total faujasite type Y– zeolite amount



produced in the first step. Finally, in the third step, the procedure under the same conditions was repeated again but on about 30 g of faujasite type Y– zeolite, which was taken from the total faujasite type Y– zeolite amount produced in the second step. The exchanged ammonia faujasite type Y– zeolites were filtered off, washed with deionized water to be free of chloride ions, dried overnight at 105°C and then calcined initially at 150°C for two hours. The temperature was increased 75°C per hour until it reached 550°C and it was held constant for 5 hours at this temperature. During calcination, ammonia and water were liberated and decationized HY– zeolite type was formed <sup>[12]</sup>.

## 2.2 : Stock solution

In order to avoid interference with other elements in hospital wastewater, the experiments in this study were carried out using simulated synthesis aqueous solutions of phenol. 1000 mg/l stock solution of phenol was prepared by dissolving 1.014 g phenol of 98.6 % purity in one liter of double distilled water. All solutions using in the experiments were prepared by diluting the stock solution with double distilled water to the desired concentrations for the experimental work of this investigation. The phenol concentrations were measured using spectrophotometer thermo – genesys 10 UV, USA.

## 2.3 Laboratory oxidation unit :

The continuous oxidation of phenol was carried out in a packed bed reactor performing co-currently up-flow. The trickle bed consists of a Stainless Steel-316 tubular reactor, 100 cm long and 2.5 cm inner diameter and controlled automatically by four sections of 15 cm height steel-jacket heaters. Independent inlet systems for gas and liquid feed allow working at various liquid to gas flow rate ratios. The liquid feed is stored in a feed tank, which is connected to a high pressure metering pump (dosing pump) that can dispense flow rates between 0 and 15 ml/min at constant pressure of 10 bars. The air oxidant comes from a high pressure cylinder equipped with a pressure controller to maintain the operating pressure constant. A flow-meter coupled with a high precision valve is used to measure and control the gas flow rate. The liquid and gas streams are mixed and then entered to the reactor at the required reaction temperature. The mixture flows along the bed packed with type faujasite Y– zeolite catalyst enclosed between two layers of inert material (also a flexible grid put at the top and bottom of the reactor to prevent fluidization of particles during the up-flow mode operation). The exited solution goes to a liquid-gas separation and sampling system, regularly, liquid samples were withdrawn for analysis. A schematic diagram of the experimental equipment is shown in **Figure.( 2)** <sup>[9]</sup>.

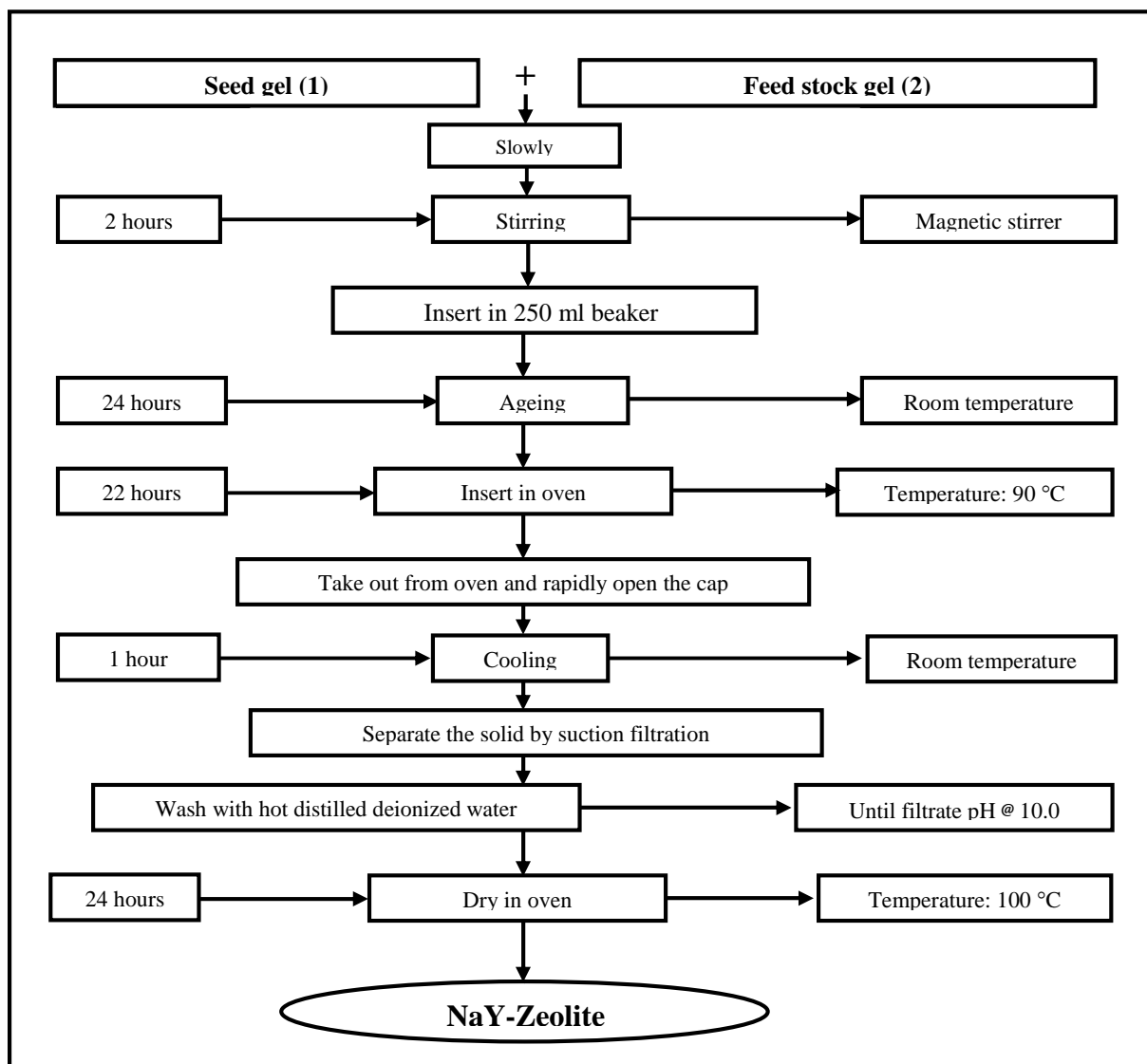


**Fig. (1): Flow Chart of Faujasite Type Y– Zeolite Catalyst Synthesis Using IRH**  
[10]

## 2.4 Catalytic Activity Test of Synthesized Catalyst :

The activity of faujasite type Y– zeolite catalyst prepared from IRH was studied by applying phenol oxidation reaction. The phenol oxidation reaction was carried out in a laboratory oxidation unit shown in **Figure. (2)** and **Figure( 3)**. This unit is operated under different conditions of reaction temperature, weight hourly space velocity (WHSV), oxygen partial pressure, pH of feed solution, phenol initial concentration, height of catalyst bed and gas flow rate aforementioned the phenol enters the reactor to pass through the catalyst layer where oxidation reaction takes place. Then products which were CO<sub>2</sub> and water will be liberated due to the reaction. Eventually, the product samples are collected and tested by spectrophotometer equipment to determine the concentration of phenol remaining.



## 2.5 Test with real hospital wastewater solution :

The ability of faujasite type Y- zeolite catalyst prepared from IRH to remove phenol by oxidation process from the real hospital wastewater solution was tested in laboratory unit at the conditions of experiment gives the best phenol percent removal from aqueous solution aforementioned which were as follow: reaction temperature = 200°C, oxygen partial pressure = 15 bar, gas flow rate = 100% stoichiometric excess, weight hourly space velocity WHSV = 1 h<sup>-1</sup>, initial concentration  $C_o = 2$  and 10 mg/l, pH = 3 and different heights of catalyst bed height ( $h = 40, 50, 60, 70$  and 80 cm). Results show that the removal efficiency for real hospital wastewater is comparable to the removal efficiency obtained for simulated synthesis aqueous solution. Experimental results obtained using real wastewater is summarized in **Figure (4)** and **Figure( 5)**.

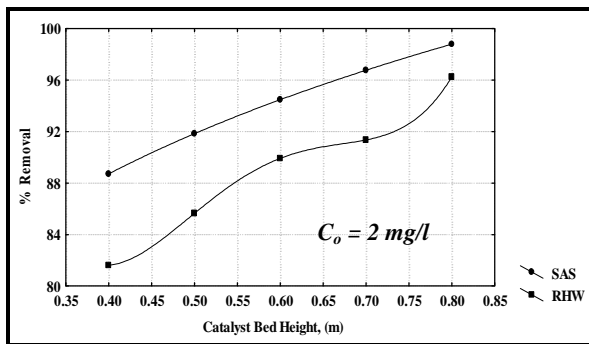


**Fig.(4): Comparison between % removal of phenol from real hospital wastewater and synthetic aqueous solution using prepared catalyst. SAS: Synthetic Aqueous Solution, RHW: Real Hospital Wastewater**

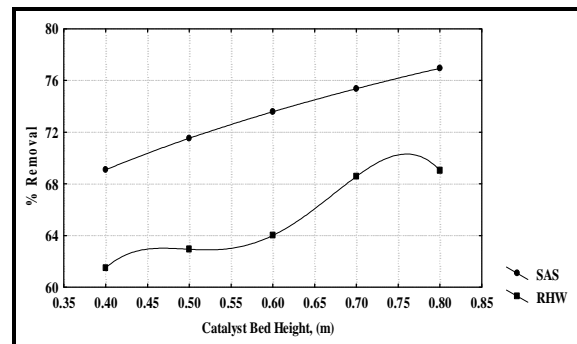


**Fig.( 5): Comparison between % removal of phenol from real hospital wastewater and synthetic aqueous solution using prepared catalyst. SAS: Synthetic Aqueous Solution, RHW: Real Hospital Wastewater**

## 3. MATHEMATICAL MODEL :

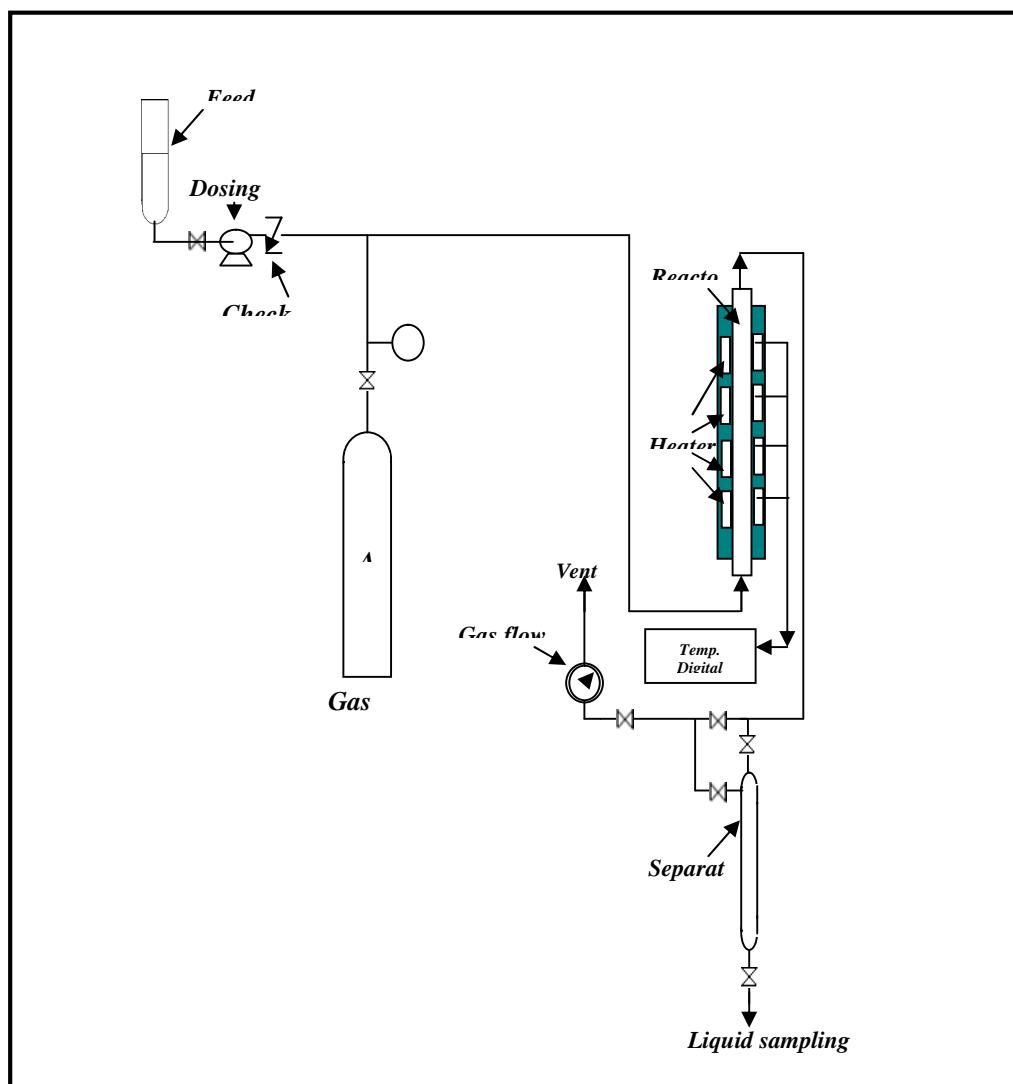
For design of oxidation process, two types of modeling approaches have been developed: the equilibrium stage model and the nonequilibrium or rate base stage model. The most difference between these two models is that the mass and heat transfer rates should be considered in every stage in the nonequilibrium stage model. For tubular reactor, the process can be simulated by equilibrium or nonequilibrium stage model [14].

### 3.1 Equilibrium Stage Model :

The schematic diagram of a  $j^{th}$  stage in the tubular reactor for equilibrium model is shown in **Figure( 6)**. In general, the assumptions [15] adopted are as operation reaches steady state, system reaches mechanical equilibrium in every stage, the vapor and liquid bulks are mixed perfectly and assumed to be at thermodynamic equilibrium and reactions take place in liquid phase. The equations that described the equilibrium stages model are known as the MESHR equations, which are listed in **Appendix A**

### 3.2 Non-Equilibrium stage model

The Non Equilibrium stage model should follow the rate-based models. The model equations of Non-Equilibrium stage for reactive distillation are similar to those for reactors. The schematic diagrams of a stage for non-equilibrium model are shown in **Figure (7)**. In general, the assumptions <sup>[15]</sup> adapted are operation reaches steady state, system reaches mechanical equilibrium in every stage, the vapor and liquid bulks are mixed perfectly and assumed non-equilibrium thermodynamic state, heat of mixing can be neglected, there is no accumulation of mass and heat at the interface, the condenser is considered as an equilibrium stage and Reactions take place in the liquid bulk within the interface. The equations that described the non-equilibrium model is listed in **Appendix B**



Fig( 2) Schematic diagram of the laboratory oxidation unit <sup>[9]</sup>

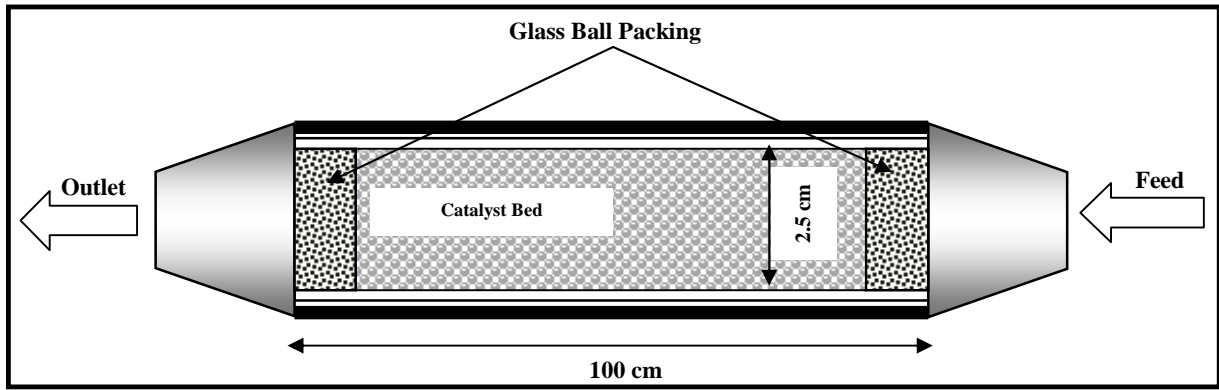


Fig (3): Schematic diagram of the laboratory oxidation unit reactor

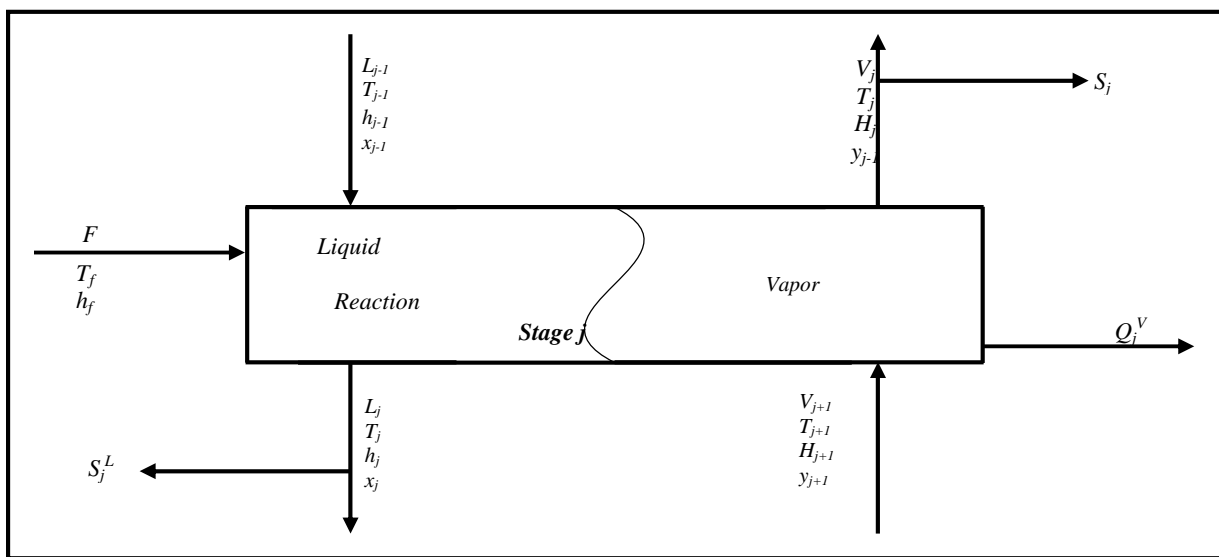


Fig (6) Schematic Diagram of an Equilibrium Stage <sup>[15]</sup>

### 3.3 Solution Procedure of the Rate Based or Non-Equilibrium Model

In order to solve the non-equilibrium or rate based model equations, a computer program using MATLAB (R2009b) has been developed to show the liquid and vapor mole fractions, interface, vapor and liquid temperatures, reaction rate profile, liquid and vapor enthalpies, liquid and vapor flow rates along stages, mass and energy transport rates for both phases and total mass flux. The rate based model program begins by specifying the model specifications and introduces the packing size and dimensions in order to be use latter in calculation of interfacial area and the mass and heat transfer coefficients. When the all specifications are given and the initial values of all operating parameters are introduce to the program, a time loop starts over all stages and the vapor and liquid flow rates are calculated using the total material balances on vapor and liquid phases respectively. Then the component material balances have been solved with the tridiagonal matrix, solving the matrices with engine value and normalizing the new mole fractions for each phase separately. Equilibrium

relation at the interface has been then used in determination of the temperature at the interface, when the summation of vapor interface mole fractions equal to 1, the temperatures of all stages are taken as the interface temperatures. Calculation of mass transfer coefficients, heat transfer coefficients and mass transfer fluxes for both phases comes next. Then, stages temperatures are estimated for each phase using the phase energy balance. Finally, reaction rate and interface mole fraction are calculated. When the iteration of time loop ended, the model results of all components are then converted to percent volume fraction for comparison with the results obtained from GC analysis of samples in experimental work.

## 4. RESULTS AND DISCUSSION

The ability of faujasite type Y– zeolite catalyst prepared from IRH to remove phenol from simulated synthesis aqueous solution by continuous oxidation unit at various parameters which were the temperature of reaction, weight hourly space velocity (WHSV), oxygen partial pressure, pH of phenol feed solution, height of catalyst bed and gas flow rate is studied in 750 experiments were achieved by varying all above parameters for five initial concentrations ( $C_o$ ) of simulated synthesis aqueous solution of phenol. Thus, the results obtained are explained below.

### 4.1 Effect of Initial Concentration

The results indicated that using faujasite type Y– zeolite catalyst prepared from IRH as a silica source, the percent removal of phenol was decreased when the initial concentration ( $C_o$ ) of simulated synthesis aqueous solution of phenol was increased at constant other variables shown in **Figure(8)**. This can be explained by the fact that the initial concentration of phenol had a restricted effect on phenol oxidation capacity; simultaneously the prepared faujasite type Y– zeolite catalyst had a limited number of active sites, which would have become saturated at a certain concentration. This was lead to the increase in the number of phenol molecules competing for the available functions groups on the surface of prepared faujasite type Y– zeolite catalyst. Since the solution of lower concentration has a small amount of phenol than the solution of higher concentration of it, so the percentage removal was decreased with increasing initial concentration of phenol. For prepared faujasite type Y– zeolite catalyst, higher percentage removal was 98.79% at initial concentration of phenol 2 mg/l, so faujasite type Y– zeolite catalyst prepared from IRH as a silica source was found to be very efficient to phenol removal from hospital wastewater.

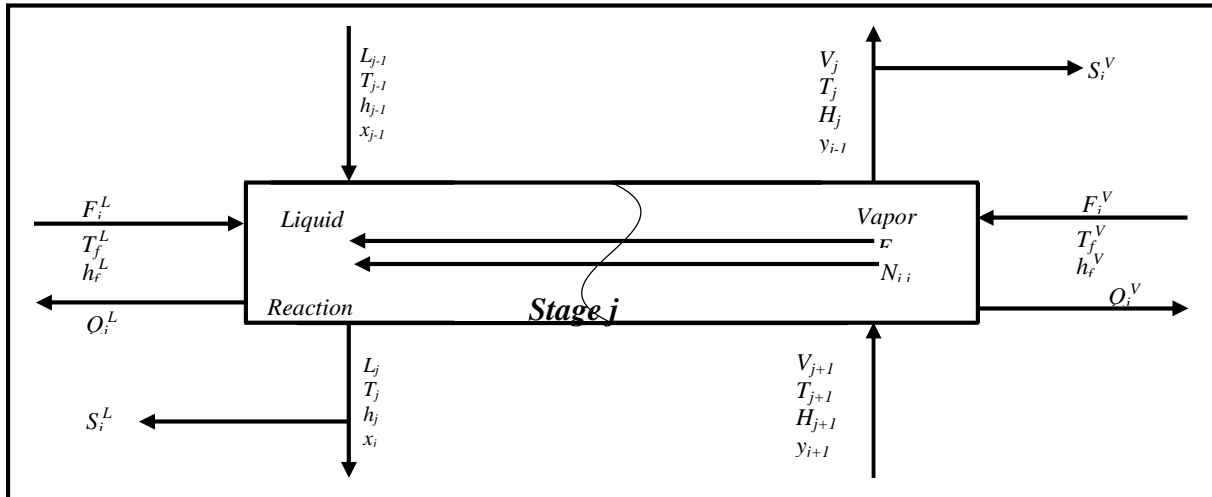


Fig.( 7) Schematic Representation of a Non-equilibrium Stage <sup>[15]</sup>

## 4.2 Effect of pH of Feed Solution

The results show that the removal of phenol using faujasite type Y– zeolite catalyst prepared from IRH as a silica source was decreased when pH of feed solution increased at constant other variables as shown in **Figure( 9)**. The variation in oxidation capacity in this pH range (3–11) is largely due to the influence of pH on the prepared faujasite type Y– zeolite catalyst characteristics of the IRH, which indicates that the oxidation capacity of the prepared faujasite type Y– zeolite catalyst is clearly pH dependent. The pH of the feed solution is an important factor that controls the removal of phenol by oxidation. pH dependence of phenol oxidation can largely be related to type and ionic state of the functional group present in the prepared faujasite type Y– zeolite catalyst and also to the chemistry of the solution. High oxidation of phenol at low pH can be explained by the fact that the oxidation reaction of phenol approved acidic environment in the trickle bed reactor, the prepared faujasite type Y– zeolite catalyst support a part of this requirement and the pH of feed solution achieved the residue part. This can be attributed to that the basic medium interferes with the acidity of catalyst during the oxidation reaction giving less active catalysts and led to restricted the acid function of it. Thus the acidity medium became low when the pH of feed solution high because the reaction need to acidic environment as mentioned above. Thus at pH = 7, the phenol conversion is slightly higher than it at pH's 9 and 11.

## 4.3 Effect of Catalyst Bed Height

The results elucidated that when the catalyst bed height was increased the percent removal of phenol was increased too at constant other variables as shown in **Figure( 10)**. The increased of catalyst bed height ( $h$ ) meaning increased in the surface area of prepared faujasite type Y– zeolite catalyst, as a result increased the number of active sites in the catalyst surface i.e. increased the availability of binding sites for adsorption and consequently increase the oxidation capacity of catalyst. This lead to increase the ability of catalyst to oxidize greater

amount of phenol from simulated synthesis aqueous solution at different initial concentrations and ultimately the percent removal of phenol increased.

#### 4.4 Effect of Gas Flow Rate

The results illustrated that when the flow rate (stoichiometric excess) of oxygen was increased, the percent removal of phenol was increased when other variables are kept constant as shown in **Figure( 11)**. This may be due to that the increasing in gas flow rate (stoichiometric excess) causing decreasing in the liquid hold up and liquid film thickness covered prepared faujasite type Y- zeolite catalyst surface, and enhancing oxygen transfer to the liquid phase, and from the liquid phase to the catalyst surface, therefore lead to high conversion of phenol to CO<sub>2</sub> and water over the catalyst surface, i.e. increasing the removal of phenol. In spite of that, increasing gas flow rate (stoichiometric excess) provides a sufficient quantity of oxygen for competitive reactions of intermediate over prepared catalyst active sites forming other undesirable compounds like p-benzoquinone and maleic acids which were both detected in high concentration in the brownish colored liquid effluent. Whatever the case may be, the conversion of phenol favor increase in oxygen flow rate but, no more than 80% (stoichiometric excess) to prevent produce undesirable side product which lower the life time of prepared faujasite type Y- zeolite catalyst.

#### 4.5 Effect of Reaction Temperature

The results demonstrated that when the reaction temperature of oxidation process was increased the percentage removal of phenol was increased when other variables are kept constant as shown in **Figure( 12)**. This may be due to the fact that at higher temperature, the kinetic constant (rate constant *K*) is favorably affected resulting an increasing in phenol conversion, according to Arrhenius equation, **equation (6)**. Also, at high temperatures in aqueous solutions, the form in which oxygen participates in chemical reactions is complex. The elevated temperatures necessary can lead to the formation of oxygen radicals, O<sup>•</sup>, which in turn can react with water and oxygen to form peroxide, H<sub>2</sub>O<sub>2</sub>, and ozone, O<sub>3</sub>, so that these four species O<sup>•</sup>, O<sub>2</sub>, O<sub>3</sub>, and H<sub>2</sub>O<sub>2</sub> are all capable of participating in the phenol oxidation.

#### 4.6 Effect of Oxygen Partial Pressure

The results implied that when the partial pressure of oxygen was increased the percent removal of phenol was increased when other variables are kept constant as shown in **Figure 13**. This may be due to the fact that in oxidation process, increasing pressure lead to increase the density of gas and increase it's solubility in the aqueous solution, therefore elevated pressure is required in such process. Also, an increasing in gas pressure may be provide a lateral push force for the reactants to cover as much surface area over catalyst as possible. In general, any increasing in oxygen partial pressure causes an increasing in phenol conversion to CO<sub>2</sub> and water over the catalyst surface, i.e. increasing the removal of phenol from aqueous solution.

#### 4.7 Effect of Weight Hourly Space Velocity (WHSV)

The results manifested that when the Weight Hourly Space Velocity (WHSV) was increased the percent removal of phenol was decreased when other variables are kept constant as shown in **Figure 14**. This may be due to reduce the space time of phenol reactant in the trickle bed reactor (i.e. reducing the time required for phenol reaction with oxygen over the catalyst). Moreover, higher liquid flow rates give greater liquid hold up which evidently decreases the contact of liquid and gas reactants at the catalyst active site, by increasing the film thickness, which lead to decrease the phenol conversion to CO<sub>2</sub> and water. While at low liquid flow rate, the liquid resides in the column for a longer time, and therefore undergoes more conversion.

#### 4.8 Characterization of Faujasite Type Y– Zeolite Catalyst

In general, the characterization of a faujasite type Y– zeolite catalyst has to provide information about structure and morphology, the chemical composition, the ability to sorbs and retain molecules and the ability to chemically convert these molecules. There are many characterization techniques but the important ones in this study are X-ray diffraction (XRD), scanning electron microscopy (SEM) and determination of BET surface area and pore volume of prepared faujasite type Y– zeolite catalyst.

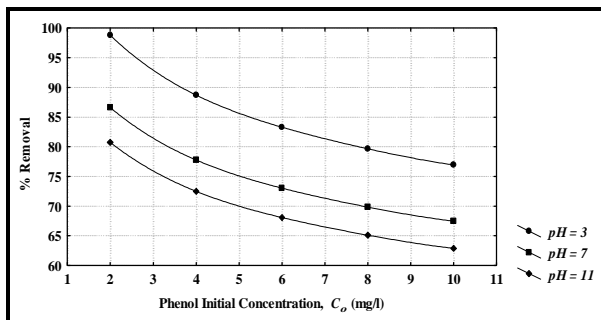


**Fig.( 8) Effect of Phenol Initial Concentration on the Percent Removal of Phenol @  $T = 200^{\circ}\text{C}$ ,  $h_{cat} = 0.8\text{m}$ ,  $G = 100\%$  S.R.,  $P = 15$  bar, and  $WHSV = 1 \text{ h}^{-1}$**

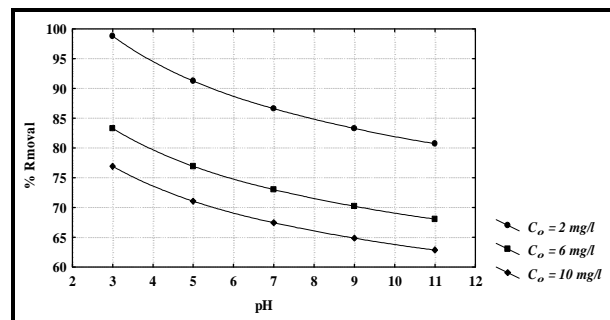


**Fig.( 9) Effect of pH on % Removal of Phenol @  $T = 200^{\circ}\text{C}$ ,  $h_{cat} = 0.8\text{m}$ ,  $G = 100\%$  S.R.,  $P = 15$  bar, and  $WHSV = 1 \text{ h}^{-1}$**



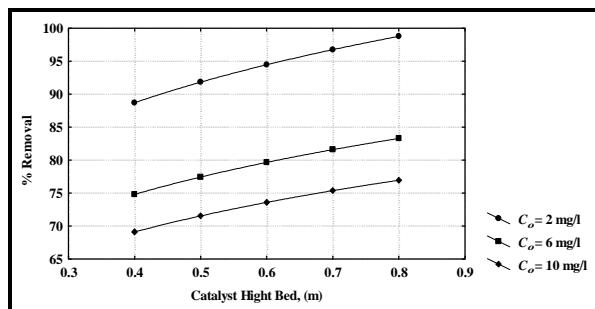


**Fig.( 10) Effect of Catalyst Bed Height on the Percent Removal of Phenol @  $T = 200^{\circ}\text{C}$ ,  $pH = 3$ ,  $G = 100\%$  S.R.,  $P = 15$  bar, and  $WHSV = 1 \text{ h}^{-1}$**

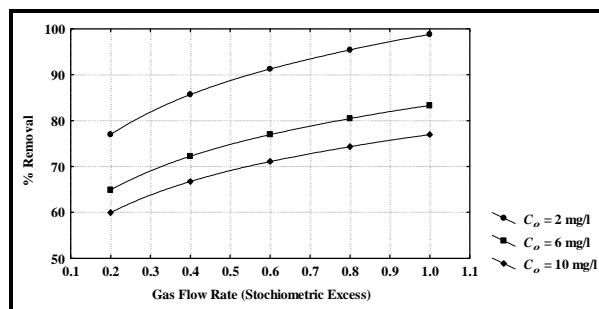


**Fig.( 11) Effect of Gas Flow Rate on the Percent Removal of Phenol @  $T = 200^{\circ}\text{C}$ ,  $h_{cat} = 0.8\text{m}$ ,  $pH = 3$ ,  $P = 15$  bar, and  $WHSV = 1 \text{ h}^{-1}$**

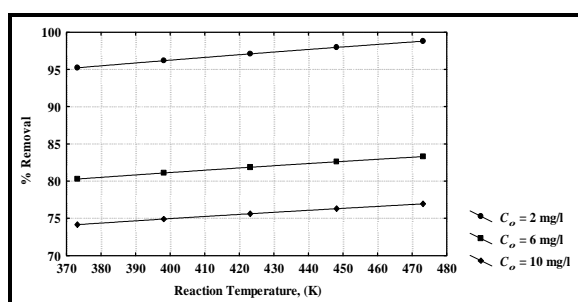


**Fig.( 12) Effect of Reaction Temperature on the Percent Removal of Phenol @  $pH = 3$ ,  $h_{cat} = 0.8\text{m}$ ,  $G = 100\%$  S.R.,  $P = 15$  bar, and  $WHSV = 1 \text{ h}^{-1}$**

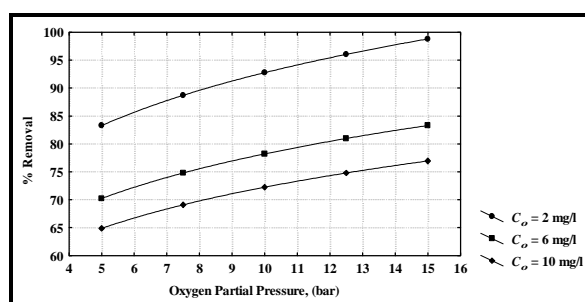


**Fig.( 13) Effect of Oxygen Partial Pressure on the Percent Removal of Phenol @  $T = 200^{\circ}\text{C}$ ,  $h_{cat} = 0.8\text{m}$ ,  $G = 100\%$  S.R.,  $pH = 3$ , and  $WHSV = 1 \text{ h}^{-1}$**

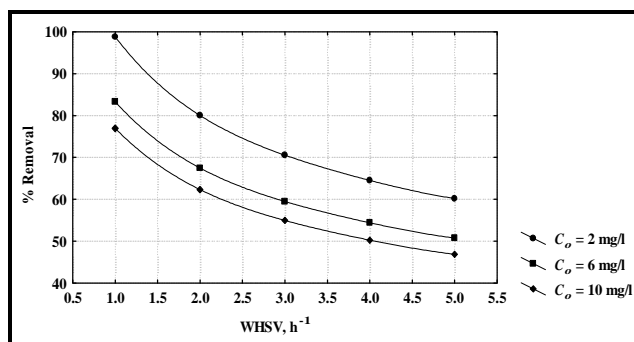


**Fig.( 14) Effect of Phenol Weight Hourly Space Velocity on the Percent Removal of Phenol @  $T = 200^{\circ}\text{C}$ ,  $h_{cat} = 0.8\text{m}$ ,  $G = 100\%$  S.R.,  $P = 15$  bar, and  $pH = 3$**

#### 4.8.1 X-Ray Diffraction (XRD)

Powder X-ray diffraction (XRD) studies were performed on the finally calcined samples in order to identify or detect different crystalline phases present in the catalyst. **Figures.(15 and 16)** illustrated XRD patterns HY-zeolite catalyst prepared from IRH. The comparison between the HY zeolite catalyst prepared and standard HY-zeolite catalyst (in mentioned

Figure) indicates that the preparation method results in a material almost compatible with the crystal structure as HY-zeolite. This leads to conclusion that the preparation method gives a nearly synthesized indigenous HY-zeolite. XRD also shows that there is small reduce in the intensity of the peaks located around differences regions, which can be explained by the prepared faujasite type Y- zeolite catalyst in addition to the nature of raw materials, which were used in the preparation method.

#### 4.8.2 Scanning Electron Microscopy (SEM)

The morphologies and crystal sizes of the synthesized HY-zeolite catalyst were observed by Leo 435VP (Variable Pressure Scanning) Zeiss-Leica Scanning Electron Microscope. The micrographs of Scanning Electron Microscopy SEM were taken in the magnification range of  $\times 20,000$  times. SEM images of HY zeolite as shown in **Figure.(17)** show that all contain particles of 20 to 50  $\mu\text{m}$  and these particles are in agglomerate form. This scanning with SEM gives the idea about particles size and their distribution also showing the way it agglomerated under the effect of Van Der Waal's forces, regarding the fact that on nanoscale the active forces become the Van Der Waals and the surface tension <sup>[17]</sup>. In fact the particles sizes affected by crystallization process in presence of structure directing agent therefore, the difference in particle sizes due to size of the nuclei formed and crystallization method progress <sup>[18]</sup> In general, the sample of HY-zeolite prepared from IRH gave a similar morphology of the crystal but with a difference in size.

#### 4.8.3 BET Surface area and pore volume

Brunauer, Emmett and Teller (BET) theory is a well known rule for the physical adsorption of gas molecules on a solid surface. The concept of the theory is an extension of the Langmuir theory. The Langmuir theory states that *the adsorbent surface is pictured as an array of  $N^s$  equivalent and independent sites for localized adsorption (one molecule per site)*. The fraction of sites occupied by  $N^a$  molecules is  $\theta = N^a/N^s$ . BET were able to extend the Langmuir mechanism to multilayer adsorption <sup>[19]</sup>. A measuring technique of specific surface area and pore volume developed on the bases of BET theory. From the kinetic theory of gases, the rate of adsorption is dependent on the pressure and the fraction of bare sites  $(1-\theta)$  which is a theory for monolayer molecular adsorption, to multilayer adsorption with the following hypotheses: *(i)* gas molecules physically adsorb on a solid in layers infinitely; *(ii)* there is no interaction between each adsorption layer; and *(iii)* the Langmuir theory can be applied to each layer. Surface area and pore volume of HY-zeolite prepared from IRH were 239.55  $\text{m}^2/\text{g}$  and 0.4235  $\text{cm}^3/\text{g}$  respectively determined by BET  $\text{N}_2$  absorption.

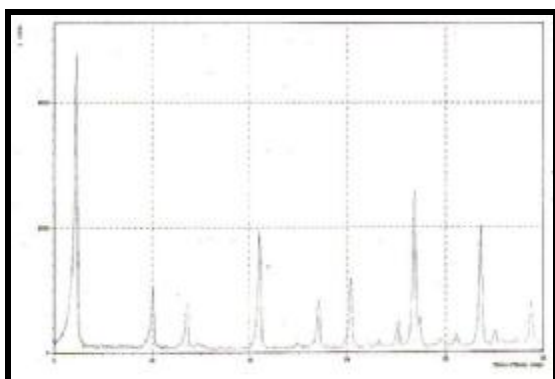


Fig.( 15) XRD pattern of prepared HY-zeolite

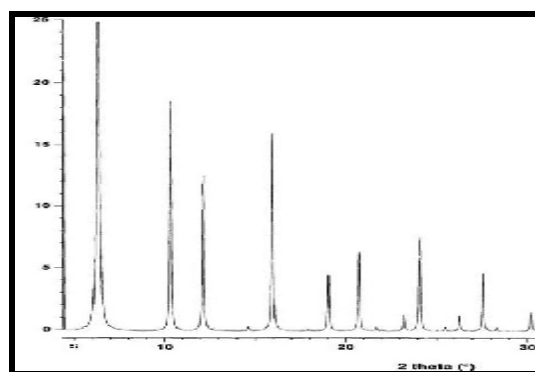


Fig.(16) Standard XRD of HY-zeolite

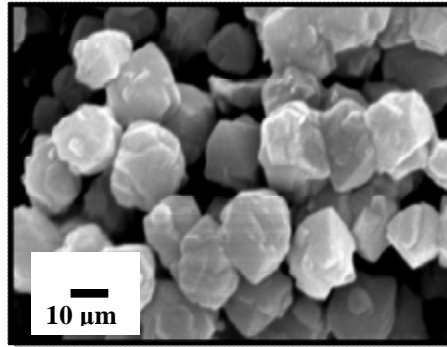


Fig.( 17) SEM of prepared HY-zeolite catalyst

#### 4.9 Comparison between the theoretical and experimental results

The model used, as described above, determines the percent removal of phenol based on different operating conditions. The results using the simulated model are compared with the experimental data obtained from phenol oxidation unit. The comparison between them is carried out in obtain deviation between experimental results and theoretical results by simulation and to find the effect of each parameter on the prediction of the results. The results predicted by proposed model show a good agreement with the experimental data with 91.53% accuracy as shown in **Figure.(18)** and **Figure.(19)**. Based on the good agreement of the model results, the deviation of the results predicted from rate based or non-equilibrium model program and the results obtained from experimental data is negligible and account within the error.

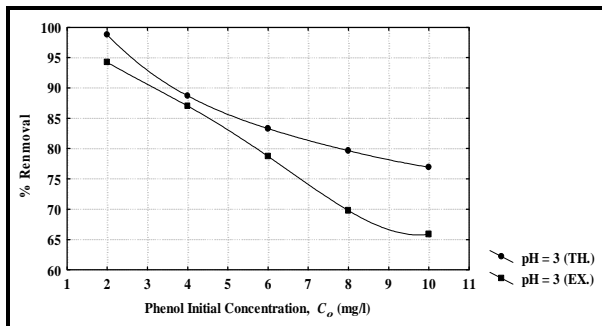


Fig.( 18) Comparison of experimental and modeling results for data obtained from oxidation unit @  $T = 200^\circ\text{C}$ ,  $h_{cat} = 0.8\text{m}$ ,  $G = 100\%$  S.R.,  $P = 15$  bar, and  $WHSV = 1 \text{ h}^{-1}$

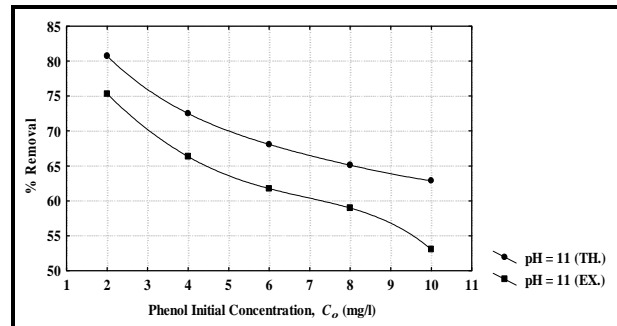


Fig.( 19) Comparison of experimental and modeling results for data obtained from oxidation unit @  $T = 200^\circ\text{C}$ ,  $h_{cat} = 0.8\text{m}$ ,  $G = 100\%$  S.R.,  $P = 15$  bar, and  $WHSV = 1 \text{ h}^{-1}$

#### 5. Statistical Model :

A statistical model was carried out on the experimental results obtained from this study. Regression Analysis and  $\pi$  Theorem was adopted to maintain a relation between the percent removal of phenol and the reaction temperature, weight hourly space velocity (WHSV), oxygen partial pressure, pH of feed solution, initial concentration of phenol, catalyst bed height and gas

flow rate. This relation is shown in equation (76), which has a correlation coefficient ( $R^2$ ) equal to 95.3%.

$$\% R = 5.556 \times 10^{-4} \frac{T^{0.1553} P^{0.1553} h^{0.1553} C_p^{0.1553} G^{0.1553}}{WHSV^{0.3106} d^{0.3106} C_o^{0.1553} pH^{0.1553} g^{0.1553}}$$

where: %R: Percent Removal Of Phenol from Aqueous Solution

*T*: Reaction Temperature, (K)

*P*: Oxygen Partial Pressure, (Pa)

*h*: Catalyst Bed Height, (m)

*C<sub>p</sub>*: Heat Capacity, (J/g.K)

*G*: Gas Flow Rate (stoichiometric excess)

*WHSV*: Weight Hourly Space Velocity, s<sup>-1</sup>

*d*: Internal Diameter of Tubular Reactor, (m)

*C<sub>o</sub>*: Initial Concentration of Phenol, (g/m<sup>3</sup>)

*g*: Gravity Acceleration, (m/s<sup>2</sup>)

## 6. Conclusions :

The following conclusions can be drawn:

- a) The maximum removal of phenol was 98.79% performed at initial concentration =2 mg/l, gas flow rate = 100% (stoichiometric excess), pH = 3, oxygen partial pressure = 15 bar, reaction temperature = 200 °C, catalyst bed height = 80 cm and WHSV = 1 h<sup>-1</sup>.
- b) The percent removal of phenol was increased with decreasing pH, WHSV and initial concentration of phenol while the percent removal was increasing with increasing reaction temperature, oxygen partial pressure, gas flow rate and the bed height of faujasite type Y- zeolite catalyst prepared from IRH.
- c) It can be prepared a good catalyst (which is faujasite type Y- zeolite) for phenol oxidation process from IRH that oxidize phenol from aqueous solution or hospital wastewater to remove the toxic waste in economic and eco-friendly method.

## 7. References :

1. Crauford, H.B. and G. Cline, 1990. Water treatment plant design.P.457 New York. American Society of Civil Engineers, American Water Work Association, McGraw Hill.
2. Fortuny, A., Ferrer, C., Bengoa, C., Font, J. and Fabregat, A., Catalysis today, 24, 79-83 (1995).
3. Fortuny, A., Font, J. and Fabregat, A., Applied Catalysis- B: Environmental, 19, 165-173 (1998).

4. Mostafa, M.R., S.E. Sarma and A.M. Yousef, 1989. Removal of organic pollutants from aqueous solution: part1, adsorption of phenol by activated carbon, *Indian J. Chem.*, 28A: 94-8 .
5. Banat, F.A., B. Al-Bashir, S. Al-Asheh and O. Hayajneh, 2000. Adsorption of phenol by bentonit. *Environmental Pollution*, 107: 391-398
6. Fortuny, A., Miro, C., Font, J. and Fabregat, A., *Catalysis today*, 48, 323-328 (1999).
7. Miro, C., Alejamdre, A., Fortuny, A., Bengoa, C. Font, J. and Fabregat, A., *Water Research*, 33, 1005-1013 (1999).
8. Pintar, A. and Levec, J., *Industrial and Engineering Chemistry Research*, 33, 3070 (1994).
9. Abdullah S. M., “Catalytic Wet Air Oxidation of Phenol in a Trickle Bed Reactor”, MSc Thesis, Baghdad University, (2007).
10. M. M. Rahman, N. Hasnida and W.B. Wan Nik, “Preparation of Zeolite Y Using Local Raw Material Rice Husk as a Silica Source”, *J. Sci. Res.* 1 (2), 285-291 (2009).
11. Mohammed Mokhtar Mohammed, F.I. Zidan and M. Thabet, “Synthesis of ZSM-5 Zeolite from Rice Husk Ash: Characterization and Implication for Photocatalytic Degradation Catalyst”, *Micropores and Mesoporous Materials*, 108 (2008) 193-203.
12. Sherman, J.D., Danner, R.P., Dranoff, J.S., and Sweed, N.H., “Adsorption and Ion Exchange Separation”, *AIChE*, 74, 179 (1978).
13. APHA, AWWA, WEF., 1995. Standard methods for the examination of water and wastewater. 19<sup>th</sup> Edn. Washington.
14. Stichlmair, J., Bravo J.L., Fair, J.R., “General Model for the Prediction of Pressure Drop and Capacity of Countercurrent Gas / Liquid Packed Columns”, *Gas Separation and Purification*, Volume 3 (1), pp. 19 – 28, (1989).
15. HATICE CEYLAN, “Control and Simulation Studies for a Multicomponent Packed Batch Distillation Column”, MSc. Thesis, The Graduate School of Natural and Applied Sciences Of Middle East Technical University, (2007)
16. Stichlmair, J., Bravo J.L., Fair, J.R., “General Model for the Prediction of Pressure Drop and Capacity of Countercurrent Gas/Liquid Packed Columns”, *Gas Separation and Purification*, Volume 3 (1), pp. 19 – 28, (1989).
17. Hari Singh Nalwa, 2002, “Nanostructured Materials and Nanotechnology”, Elsevier Inc.
18. Eric G. Derouane, 2006, “Microporous and Mesoporous Solid Catalysts”, John Wiley & Sons Ltd. Françoise Rouquerol, Jean Rouquerol and Kenneth Sing, 1999, “Adsorption by Powders and Porous Solids Principles, Methodology and Applications”, Elsevier Ltd.
19. Françoise Rouquerol, Jean Rouquerol and Kenneth Sing, 1999, “Adsorption by Powders and Porous Solids Principles, Methodology and Applications”, Elsevier Ltd.

**Appendix A**

$$\frac{dM_j}{dt} = V_{j+1} + L_{j-1} + F_j - (1 + r_j^V) V_j - (1 + r_j^L) L_j + \sum_{k=1}^r \sum_{i=1}^c v_{i,k} R_{k,j} e_j \quad (1)$$

$$\frac{dM_j x_{i,j}}{dt} = V_{j+1} y_{i,j+1} + L_{j-1} x_{i,j-1} + F_j z_{i,j} - (1 + r_j^V) V_j y_{i,j} - (1 + r_j^L) L_j x_{i,j} + \sum_{k=1}^r \sum_{i=1}^c v_{i,k} R_{k,j} e_j \quad (2)$$

$$y_{i,j} = K_{i,j} x_{i,j} \quad (3)$$

$$\sum_{i=1}^c x_{i,j} = 1, \quad \sum_{i=1}^c y_{i,j} = 1 \quad (4)$$

$$\frac{dM_j H_j}{dt} = V_{j+1} H^V_{j+1} + L_{j-1} H^L_{j-1} + F_j H^F_j - (1 + r_j^V) V_j H^V_j - (1 + r_j^L) L_j H^L_j - Q_j + R_j H_r \quad (5)$$

$$r_{Phenol} = \frac{dC_{Phenol}}{dt} = k C_{Phenol}, \quad k = A \exp\left(\frac{-E_a}{RT}\right) \quad (6)$$

**Appendix B**

$$\frac{dM_{i,j}^V}{dt} = V_{j+1} y_{i,j+1} - V_j y_{i,j} + z_{i,j}^V F_{i,j}^V - N_{i,j}^V \quad (7)$$

$$\frac{dM_{i,j}^L}{dt} = L_{j-1} x_{i,j-1} - L_j x_{i,j} + z_{i,j}^L F_{i,j}^L - N_{i,j}^L + \sum_{k=1}^r v_{i,k} R_{j,k} e_j^L \quad (8)$$

$$\frac{dM_j^V}{dt} = V_{j+1} - V_j + F_{i,j}^V - \dot{a} \sum_{k=1}^c N_{k,j}^V \quad (9)$$

$$\frac{dM_j^L}{dt} = L_{j-1} - L_j + F_{i,j}^L - \sum_{k=1}^c N_{k,j}^L + \sum_{i=1}^c \sum_{k=1}^r v_{i,k} R_{k,j} e_j^L \quad (10)$$

$$y_{i,j} = \frac{M_{i,j}^V}{M_j^V}, \quad x_{i,j} = \frac{M_{i,j}^L}{M_j^L} \quad (11)$$

$$\sum_{i=1}^c x_{i,j} = 1, \quad \sum_{i=1}^c y_{i,j} = 1 \quad (12)$$

$$\frac{dE_j^V}{dt} = V_{j+1} H^V_{j+1} - V_j H^V_j + F_j^V H^V_j - E_j^V - Q_j^V \quad (13)$$

$$\frac{dE_j^L}{dt} = L_{j-1} H^L_{j-1} - L_j H^L_j + F_j^L H^L_j + E_j^L - Q_j^L \quad (14)$$

$$\frac{x_i^L}{RT^L} \frac{\partial m_i^L}{\partial h} = \dot{a} \sum_{k=1}^c \frac{x_i^L N_k^L - x_k^L N_i^L}{C_i^L D_{i,k}^L} \quad (15)$$

$$\frac{y_i^V}{RT^V} \frac{\partial m_i^V}{\partial h} = \sum_{k=1}^c \frac{y_i^V N_k^V - y_k^V N_i^V}{C_i^V D_{i,k}^V a} \quad (16)$$

$$\sum_{i=1}^c x^{i,L} = 1, \quad \sum_{i=1}^c y^{i,V} = 1 \quad (17)$$

$$E^{i,L} = -h^{i,L} A \frac{\partial T^{i,L}}{\partial h} + \sum_{i=1}^c N^{i,L} H_i^{i,L} \quad (18)$$

$$y_{i,j} \Big|_I = K_{i,j} x_{i,j} \Big|_I \quad (19)$$

$$N_i^{iV} = N_i^{iL}, \quad E_i^{iV} = E_i^{iL} \quad (20)$$

$$h_i = \Delta H_{f,i}^{298} + \int_{298}^T C_{p_i}^L dT \quad (21)$$

$$Cp_i^L = a + bT + cT^2 + dT^2 \quad (22)$$

$$h_{i,j} = \sum_{i=1}^c x_{i,j} h_i + H_{mix} \quad (23)$$

$$H_{mix} = R T \sum_{i=1}^c (x_i \ln g_i) \quad (24)$$

$$\Delta H_i = \int_{T^o}^T Cp_i^V dT \quad (25)$$

$$Cp_i^V = A + BT + CT^2 + DT^2 \quad (26)$$

$$H_{i,j}^V = y_{i,j} H_i \quad (27)$$

$$H_r = H_r^o \int_{T^o}^T \Delta Cp_i^V dT \quad (28)$$

$$\ln g_i = \ln g_i^c + \ln g_i^r \quad (29)$$

$$\ln g_i^c = 1 - J_i + \ln J_i - 5 q_i \left(1 - \frac{J_i}{L_i} + \ln \frac{J_i}{L_i}\right) \quad (30)$$

$$\ln g_i^r = q_i \left[1 - \sum_k \left(q_k \frac{b_{ik}}{S_k} - e_{ki} \ln \frac{b_{ik}}{S_k}\right)\right] \quad (31)$$

$$J_i = \frac{r_i}{\sum_j r_j x_j} \quad (32)$$

$$L_i = \frac{q_i}{\sum_j q_j x_j} \quad (33)$$

$$S_i = \sum_j q_m t_{mi} \quad (34)$$

$$r_i = \sum_k u_k^{(i)} R_k \quad (35)$$

$$q_i = \sum_k u_k^{(i)} Q_k \quad (36)$$

$$b_{ik} = \sum_m e_{mi} t_{mk} \quad (37)$$

$$q_k = \frac{\sum_i x_i q_i e_{ki}}{\sum_j x_j q_j} \quad (38)$$

$$t_{mk} = \exp \frac{a_{mk}}{T} \quad (39)$$

$$f = \exp \left[ \frac{Pr}{T_r} (B^o + w B') \right] \quad (40)$$

$$B^o = 0.083 - \frac{0.422}{T_r^{1.6}} \quad (41)$$

$$B' = 0.139 - \frac{0.172}{T_r^{4.2}} \quad (42)$$

$$\ln P_i^{sat} = A - \frac{B}{C + T} \quad (43)$$

$$\sum_{i=1}^m (K_{i,j} x_{i,j}) = 1 \quad (44)$$

$$K = g_i \frac{P_i^{sat}}{P} \quad (45)$$

$$\frac{\Delta P}{z} = \frac{3}{4} f_o \left[ \frac{(1 - e)}{e^{465}} \right]^{d_p \frac{r_o u_o^2}{d_p}} \quad (46)$$



$$f_o = \frac{C_1}{Re_g} + \frac{C_2}{Re_g^{0.5}} + C_3 \quad (47)$$

$$C = \frac{\frac{C_1}{Re_g} - \frac{C_2}{(2 Re_g^{0.5})}}{f_o} \quad (48)$$

$$M = \frac{1}{12} \frac{\alpha m_L \bar{\omega}^{1/6}}{e \xi r_L \bar{\omega}} (\mu_L a_p)^{0.5} \quad (49)$$

$$N_{ij}^V = a_j^I J_{ij}^V + y_{ij} N_j^T \quad (50)$$

$$N_{ij}^L = a_j^I J_{ij}^L + x_{ij} N_j^T \quad (51)$$

$$J_{ij}^V = C_t^V [k^V] (y_{ij} - y_{ij}^I) \quad (52)$$

$$J_{ij}^L = C_t^L [k^L] (x_{ij} - x_{ij}^I) \quad (53)$$

$$N_j^V = C_{ij}^V [k^V] a_j (y_{ij} - y_{ij}^I) + y_{ij} N_j^{TV} \quad (54)$$

$$N_j^L = C_{ij}^L [k^L] a_j (x_{ij} - x_{ij}^I) + x_{ij} N_j^{TL} \quad (55)$$

$$[k^V] = [R^V]^{-1} \quad (56)$$

$$[k^L] = [R^L]^{-1} [\Gamma^L] \quad (57)$$

$$R_{il,j} = \frac{y_{ij}}{k_{i,nc} a_j} + \sum_{\substack{k \neq 0 \\ k=1}}^{nc} \frac{y_{k,j}}{k_{ik,j} a_j} \quad (58)$$

$$R_{il,j} = -y_{ij} + \left( \frac{1}{k_{il,j} a_j} - \frac{1}{k_{inc,j} a_j} \right) \quad (59)$$

$$\Gamma_{ik,j} = d_{ik,j} + x_{ij} \left( \frac{\partial \ln g_{ij}}{\partial x_{kj}} \right) \quad (60)$$

$$e_j^V = a_j^I h^V (T^V - T^I) + E_j^V \quad (61)$$

$$e_j^L = a_j^I h^L (T^L - T^I) + E_j^L \quad (62)$$

$$E_j^V = \sum_{i=1}^{nc} N_{ij}^V H_{ij}^V \quad (63)$$

$$E_j^L = \sum_{i=1}^{nc} N_{ij}^L H_{ij}^L \quad (64)$$

$$k^V = A Re_v^{0.7} Sc_v^{0.333} (a_p D^V) (a_p d_p)^{-2} \quad (65)$$

$$k^L = 0.0051 (Re_L^I)^{2/3} Sc_v^{-0.5} (a_p d_p)^{0.4} (m^L g / r^L)^{1/3} \quad (66)$$

$$Re_L^I = \frac{r^L u^L}{m^L a_d} \quad (67)$$

$$a_d = 0.498 (C_{aL} Re_v)^{0.392} s^{0.5} H^{-0.4} a_p \quad (68)$$

$$C_{aL} = \frac{a^L m^L}{r^L s} \quad (69)$$

$$D_{ik,j}^L = (D_{ik,j}^o)^{x_{ij}} (D_{ik,j})^{x_{kj}} \quad (70)$$

$$D_{ik,j}^o = 117.4 \times 10^{-8} \frac{(j_k M_k)^{1/2}}{m_{kj}^L V_i^{0.6}} \quad (71)$$

$$D_{ik,j}^V = \frac{0.1014 (T^V)^{1.5} \left( \frac{1}{M_i} + \frac{1}{M_k} \right)^{0.25}}{p \left( V_i^{1/3} + V_k^{1/3} \right)^2} \quad (72)$$

$$h^V = k^V r^V Cp^V (N_{Le}^V)^{2/3} \quad (73)$$

$$N_{Le}^V = \frac{Sc^V}{N_{Pr}^V} \quad (74)$$

$$h^L = k^L r^L Cp^L (N_{Le}^L)^{1/2} \quad (75)$$